



**HAL**  
open science

## Bottom-Up Electrochemical Fabrication of Conjugated Ultrathin Layers with Tailored Switchable Properties

Verena Stockhausen, van Quyen Nguyen, Pascal G.P. Martin, Jean Christophe Lacroix

► **To cite this version:**

Verena Stockhausen, van Quyen Nguyen, Pascal G.P. Martin, Jean Christophe Lacroix. Bottom-Up Electrochemical Fabrication of Conjugated Ultrathin Layers with Tailored Switchable Properties. ACS Applied Materials & Interfaces, 2017, 9 (1), pp.610-617. 10.1021/acsami.6b08754 . hal-01821774

**HAL Id: hal-01821774**

**<https://u-paris.hal.science/hal-01821774>**

Submitted on 25 Jun 2018

**HAL** is a multi-disciplinary open access archive for the deposit and dissemination of scientific research documents, whether they are published or not. The documents may come from teaching and research institutions in France or abroad, or from public or private research centers.

L'archive ouverte pluridisciplinaire **HAL**, est destinée au dépôt et à la diffusion de documents scientifiques de niveau recherche, publiés ou non, émanant des établissements d'enseignement et de recherche français ou étrangers, des laboratoires publics ou privés.

This document is confidential and is proprietary to the American Chemical Society and its authors. Do not copy or disclose without written permission. If you have received this item in error, notify the sender and delete all copies.

### **Bottom-Up Electrochemical Fabrication of Conjugated Ultrathin Layers with Tailored switchable properties**

Journal:	<i>ACS Applied Materials &amp; Interfaces</i>
Manuscript ID	am-2016-08754q
Manuscript Type:	Article
Date Submitted by the Author:	31-Aug-2016
Complete List of Authors:	Stockhausen, Verena; University Paris 7-Debis Diderot, Chimie Nguyen , Van ; University Paris 7-Denis Diderot, ITODYS Martin, Pascal; University Paris 7, Chemistry Lacroix, Jean-Christophe; University Paris 7-Denis Diderot, ITODYS

SCHOLARONE™  
Manuscripts

# Bottom-Up Electrochemical Fabrication of Conjugated Ultrathin Layers with Tailored switchable properties

*Verena Stockhausen<sup>1</sup>, Van Quyen Nguyen<sup>1,2</sup>, Pascal Martin<sup>1</sup>, Jean Christophe Lacroix<sup>1\*</sup>*

<sup>1</sup>Université Paris Diderot, Sorbonne Paris Cité, ITODYS, UMR 7086 CNRS, 15 rue Jean-Antoine de Baïf, 75205 Paris Cedex 13, France.

<sup>2</sup> Department of Advanced Materials Science and Nanotechnology, University of Science and Technology of Hanoi (USTH), Vietnam Academy of Science and Technology, 18 Hoang Quoc Viet, Cau Giay, Hanoi, Vietnam

**KEYWORDS.** Bottom-up approach, nano-electrochemistry, ultrathin film,  $\pi$ -conjugated material, diazonium grafting, molecular electronics.

**ABSTRACT:** In this work, we develop a Bottom-Up Electrochemical Fabrication process of Conjugated Ultrathin Layers with Tailored switchable properties. To do so, we use ultrathin layers of covalently grafted oligo(bisthienylbenzene) (oligo(BTB)) as a switchable organic electrodes and perform 3,4-ethylenedioxythiophene (EDOT) oxidation on such organic layer. Adding only 3 nm of EDOT moieties (5 to 6 units) completely changes the switching properties of the layer without changing the surface concentration of the grafted electroactive species. As a consequence, a range of new materials, with tunable interfacial properties, is created through this bottom-up electrochemical process. They consist of oligo(BTB)-oligo(EDOT) di-block oligomers of various relative length grafted covalently on the underlying electrode. As an

1  
2  
3 important result these ultrathin films retain reversible redox *on/off switching* and their switching  
4  
5 potential can be finely tuned between 0.6 and -0.3 V/SCE despite an overall thickness that  
6  
7 remains below 11 nm.  
8  
9

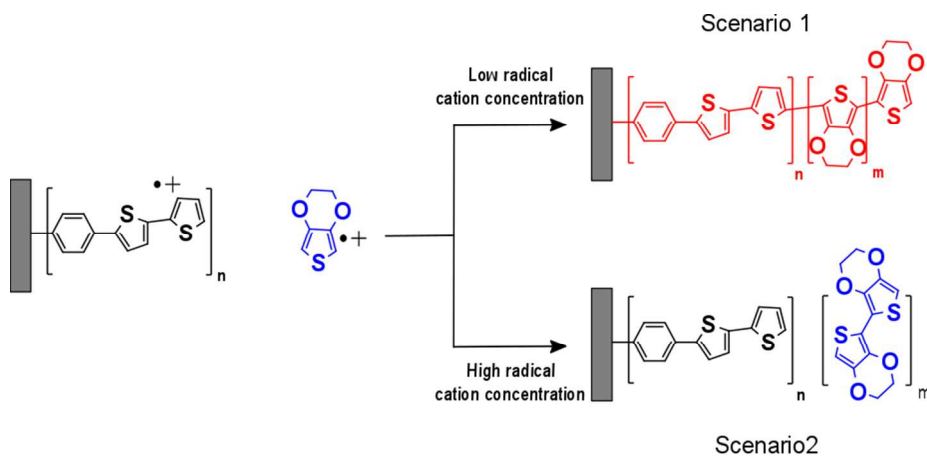
## 10 11 12 INTRODUCTION

13  
14  
15  
16 Bottom-up approach is one of the heart pieces of modern material science and provides  
17  
18 an enormous creativity in its use as tool for the fabrication of an almost undetermined choice of  
19  
20 smart materials<sup>1-6</sup>, interfaces<sup>4, 6-14</sup> and nanoelectronic devices<sup>15-24</sup>. Ultrathin films of conjugated  
21  
22 oligomers grafted on surfaces from diazonium salt reduction are of particular interest for the  
23  
24 fabrication of molecular electronic devices<sup>17, 25-27</sup>. Indeed they allow the fabrication in high yield  
25  
26 of robust molecular junctions using CMOS compatible processes<sup>25-26</sup>. Among such layers,  
27  
28 ultrathin films combining thiophene and EDOT units exhibit unique on/off switching of their  
29  
30 transport properties in electrochemical environment<sup>28-31</sup>. Insulating behavior is observed below  
31  
32 an intrinsic film commutation potential whereas above this potential, they become conductive.  
33  
34 As a consequence, reversible redox probes with an  $E^0$  below this intrinsic film commutation  
35  
36 potential exhibit an anodic peak shifted towards higher potential and no cathodic peak, while  
37  
38 reversible redox probes with an  $E^0$  above the film commutation potential exhibit the same redox  
39  
40 behaviour as on bare electrodes<sup>28-29</sup>. The film commutation potential depends on the molecular  
41  
42 structure of the grafted oligomers and incorporating EDOT in the molecular backbone decreases  
43  
44 the layer switching potential<sup>28, 30</sup>. Overall, such systems combine the advantages of conductive  
45  
46 oligomers to those of diazonium based layers, i.e. fine control of the film thickness in the 2 to 20  
47  
48 nm range, ability to generate robust, pinhole free and electroactive layers, two redox states of  
49  
50 different conductivity<sup>26</sup>. As a consequence they can be seen as switchable organic electrodes.  
51  
52  
53  
54  
55  
56  
57  
58  
59  
60

1  
2  
3  
4  
5  
6  
7  
8  
9  
10  
11  
12  
13  
14  
15  
16  
17  
18  
19  
20  
21  
22  
23  
24  
25  
26  
27  
28  
29  
30  
31  
32  
33  
34  
35  
36  
37  
38  
39  
40  
41  
42  
43  
44  
45  
46  
47  
48  
49  
50  
51  
52  
53  
54  
55  
56  
57  
58  
59  
60

In this work we investigate a bottom-up electrochemical process based on the electrochemical oxidation of irreversible redox systems on such a switchable organic electrodes, namely oligo(bisthienylbenzene) (BTB) layer. In doing so, we wish to create new ultrathin layers with tunable properties. For this purpose, we chose to study EDOT oxidation, a monomer whose oxidation is irreversible, gives unstable EDOT radical cations and yields on a bare electrode to PEDOT deposition. As EDOT oxidation potential is located beyond the switching potential of the grafted oligo(BTB), it will take place on a p-doped organic conductive electrode, that is a layer in which oligo(BTB) radical cations are already generated. As a consequence, two types of reactive radical cations will be created in the vicinity of the electrode and we will investigate the outcome of their chemical coupling and the resulting electrode modification. In doing so we wish to evaluate if it is possible to extend the ways to combine the advantages of conductive oligomers to those of diazonium based layers using a low cost bottom up nano-electrochemical process.

Scheme 1 displays the two possible scenarios and materials that can be expected, depending on the concentration of the EDOT radical cations generated in the vicinity of the oligo(BTB) electrode and their relative reactivity towards oligo(BTB) radical cations.



1  
2  
3 **Scheme 1:** Alternative scenarios that can be anticipated when performing EDOT  
4 oxidation on an oligo(BTB) layer. In scenario 1, a new material is generated by covalent  
5 attachment of EDOT on oligo(BTB). In scenario two, Oligo(BTB) layer is covered by PEDOT  
6 and an interface exists between the two materials  
7

8  
9 First, at low EDOT radical cation concentration (*i.e.*; low EDOT oxidation current  
10 density), EDOT radical cations can couple covalently to the grafted layer and thus extend the  
11 aromatic chain and create new block oligomers with new properties (Scenario 1). In this case, a  
12 new material is generated and its electrochemical and interfacial properties differ from those of  
13 the initial BTB layer.  
14  
15  
16  
17  
18  
19

20  
21 Alternatively, at high current densities, EDOT radical cations may prefer to react with  
22 each other and form oligomers in solution or even a polymer. It can then precipitate onto the first  
23 layer, yielding a double layer structure by physisorption (Scenario 2). In this case, two different  
24 materials are deposited in a bilayer structure with a specific interface separating the two  
25 materials. As the BTB layer is not modified in this scenario, it keeps its electrochemical  
26 properties. As BTB potential switch is above that of PEDOT, BTB will command the  
27 electrochemical properties of the physisorbed PEDOT layer.  
28  
29  
30  
31  
32  
33  
34  
35  
36  
37  
38

## 39 **EXPERIMENTAL METHODS**

40  
41  
42 *Chemicals:* 1-(2-bisthienyl)-4-aminobenzene were synthesized according to published  
43 procedures<sup>28, 32</sup>. All chemicals were used as received. Ferrocene (Fc), decamethylferrocene  
44 (DmFc) and were purchased from Sigma Aldrich. Tert-butyl nitrite (tBuO-NO) was purchased  
45 from Aldrich. Lithium perchlorate (LiClO<sub>4</sub>) and tetrabutylammonium tetrafluoroborate  
46 (Bu<sub>4</sub>NBF<sub>4</sub>) from Aldrich were used as supporting electrolyte at 0.1 M concentration in  
47 acetonitrile (ACN). 3,4-ethylenedioxythiophene (EDOT) was from Bayer.  
48  
49  
50  
51  
52  
53  
54  
55  
56  
57  
58  
59  
60

1  
2  
3 *Electrochemical deposition of the oligo(BTB) layer:* The *in situ* formation of the diazonium  
4 cation from 1-(2-bisthienyl) precursor was performed without any acid in the solution, by adding  
5 tert-butyl nitrite (tBuO-NO)<sup>28, 33-35</sup> Briefly, an acetonitrile solution containing of 1-(2-  
6 bisthienyl)-4-aminobenzene (0.5 mM) and Bu<sub>4</sub>NBF<sub>4</sub> (0.1 M) as supporting electrolyte was  
7 prepared and degassed by argon bubbling for at least 10 min. Following that, tBuO-NO was  
8 added in excess to the solution (30 equivalents). As the reaction between amine function and tert-  
9 butyl nitrite is relatively slow, grafting was only started after 5 minutes incubation time. BTB  
10 layer deposition was performed using multicycle voltammetry between 0.4 V/SCE and -0.4  
11 V/SCE on glassy carbon electrodes as well as on gold stripes (20 μm wide and 5 mm long). The  
12 thickness of the deposited layer was measured using tapping mode AFM and was set to ~8 nm.  
13 Each electrode was then characterized in acetonitrile containing 1 mM ferrocene and 0.1 M  
14 LiClO<sub>4</sub>.

15  
16  
17  
18  
19  
20  
21  
22  
23  
24  
25  
26  
27  
28  
29  
30  
31  
32 *Electrochemical oxidation of EDOT on the oligo(BTB) organic electrode:* Electrodes previously  
33 functionalized by oligo(BTB) were sonicated in ACN for 10 minutes and plunged in a solution  
34 containing 2 x 10<sup>-2</sup> M EDOT. Cyclic voltammograms were performed while the potential  
35 window was adjusted in order to obtain oxidation charges turning around 0.3 mC/cm<sup>2</sup>,  
36 corresponding to a maximal theoretical deposition thickness of 2 nm for each EDOT oxidation  
37 cycle (or around 3-4 moieties, considering a size of 0.6 nm per EDOT unit). After each oxidation  
38 cycle, the electrode was thoroughly rinsed with ACN and electrochemically characterized in  
39 electrolyte solution (0.1 M LiClO<sub>4</sub> in ACN), without any redox probe, at a scan rate of 10 V/s  
40 (with ohmic drop compensation). Then, voltammograms in presence of Fc and DmFc were  
41 recorded using the same modified electrode. This procedure (EDOT deposition on the organic  
42  
43  
44  
45  
46  
47  
48  
49  
50  
51  
52  
53  
54  
55  
56  
57  
58  
59  
60

1  
2  
3 electrode, rinsing characterisation in Fc, and DmFc, and in redox probe free solution) was  
4 repeated several times.  
5  
6

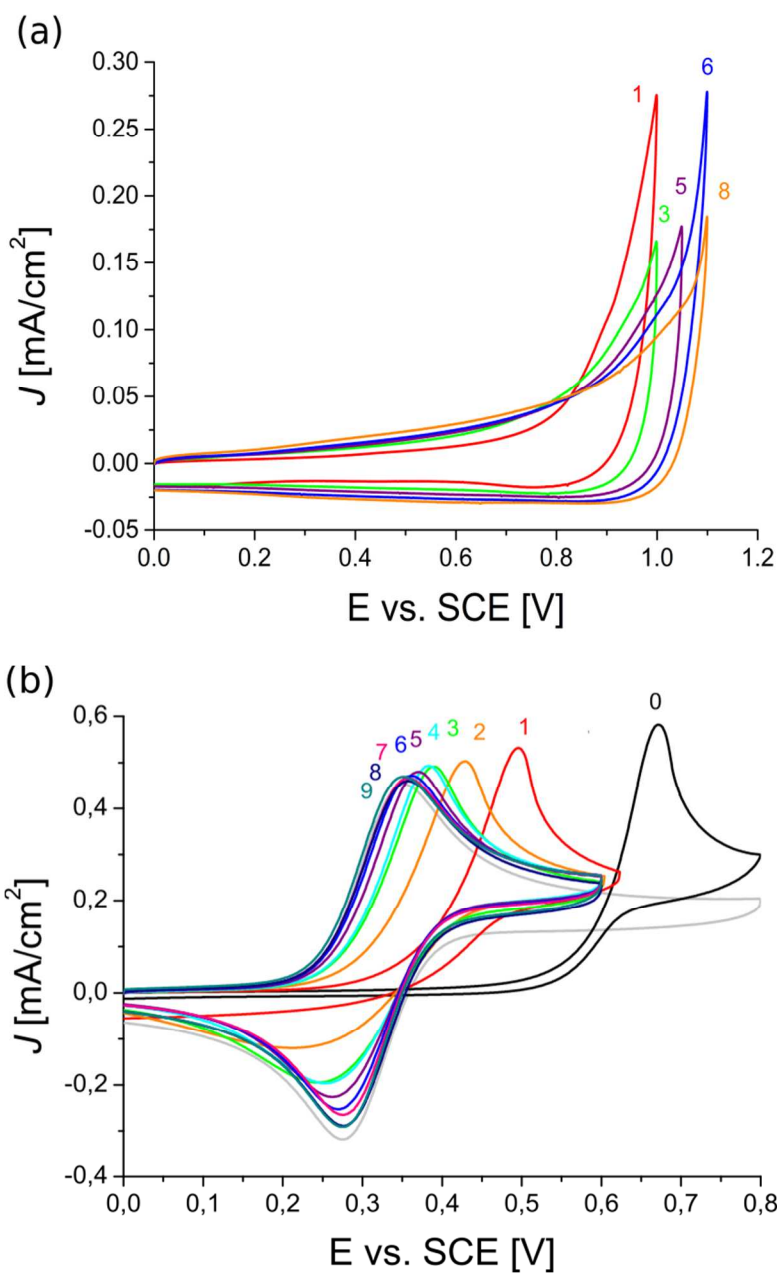
7  
8  
9 *AFM characterization:* AFM measurements were performed on a Molecular Imaging system  
10 (picoscan 5500). AFM images are recorded in tapping mode with tapping tip from Budgetsensor  
11 (AFM tap 300G, resonant freq 300kHz, force constant 40nN/m). Blank studies were first realized  
12 on bare Au microelectrode in order to measure the thickness of Au stripes. The thickness of the  
13 grafted layer is then determined by subtracting the thickness of the Au bottom electrode<sup>26, 36</sup>.  
14  
15  
16  
17  
18  
19

## 20 21 22 **RESULTS AND DISCUSSION**

23  
24  
25 The voltammograms of EDOT oxidation onto the BTB layer are shown in Figure 1a,  
26 where the number of cycles used is indicated. EDOT oxidation onset starts at 0.8 V/SCE and is  
27 as expected irreversible. Successive oxidation cycles show that this onset shifts slightly to higher  
28 values as the BTB layer is modified by EDOT moieties deposition. In order to generate a small  
29 amount of EDOT radical-cations, the current density has been restricted to be below 0.3  
30 mA/cm<sup>2</sup>. EDOT oxidation is here performed at the threshold of the EDOT oxidation signal  
31 which can reach current as high as 20 mA/cm<sup>2</sup> with such EDOT concentration. After each  
32 oxidation cycle, the electrode was thoroughly rinsed with ACN and electrochemically  
33 characterized in electrolyte solution (0.1 M LiClO<sub>4</sub> in ACN), with Fc then with DmFc redox  
34 probe. Voltammograms of Fc and DmFc were recorded using the **same modified electrode**. The  
35 electrochemical responses of these two redox probes are thus an indication of the modifications  
36 of the layer electrochemical properties, induced by each EDOT deposition cycle. This procedure  
37 (EDOT deposition on the organic electrode, rinsing characterisation in Fc, and DmFc,) was  
38  
39  
40  
41  
42  
43  
44  
45  
46  
47  
48  
49  
50  
51  
52  
53  
54  
55  
56  
57  
58  
59  
60

repeated several times in order to monitor the progressive evolution of the transport properties of the modified electrode.

Figure 1b and 1c illustrate the evolution of Fc and DmFc voltamograms on such BTB based organic electrodes as a function of the number of EDOT oxidation cycles used to modify the initial BTB electrode.



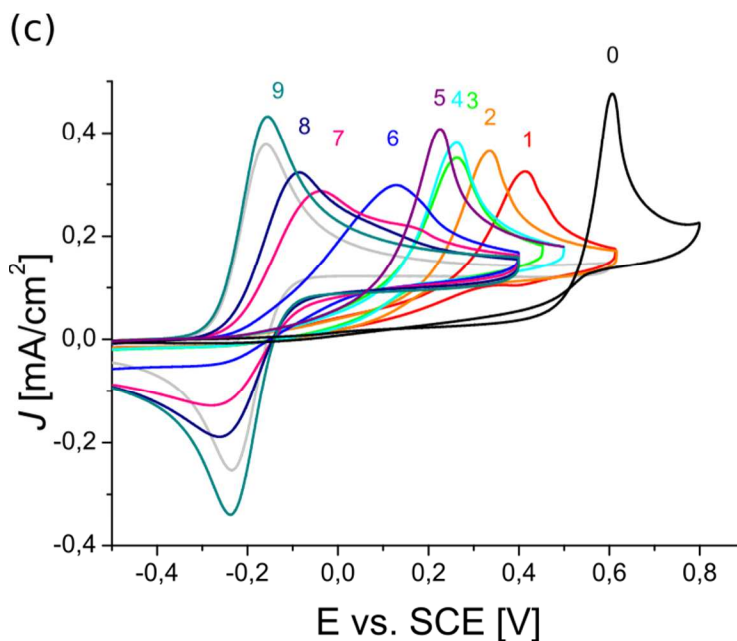


**Figure 1:** (a) EDOT oxidation on a oligo(BTB)-modified GC electrode in ACN with EDOT ( $2 \times 10^{-2}$  M) and  $\text{LiClO}_4$  (0.1 M); (b) Response of ferrocene on the oligo(BTB)/EDOT modified electrodes (Fc; 1 mM) with  $\text{LiClO}_4$  (0.1 M) as supporting electrolyte in ACN, after cycling in EDOT solution ( $2 \times 10^{-2}$  M). 0 represents Fc response prior to EDOT cycling, 1-9 represent the number of deposition cycles in EDOT solution used for modifying the BTB electrode. (c) Response of decamethylferrocene on the same oligo(BTB)/EDOT modified electrodes (dmFc; 1 mM) with  $\text{LiClO}_4$  (0.1 M) as supporting electrolyte in ACN, after cycling in EDOT solution ( $2 \times 10^{-2}$  M). 0 represents electrode response prior to EDOT cycling, 1-9 represent the number of deposition cycles. Scan rate: 0.1 V/s.

Ferrocene oxidation signal on the initial oligo(BTB) layer is curve labelled “0”. As ferrocene redox potential is below the switching potential of the oligo(BTB) layer, it has a typical diode like signature, *i.e.* no current is observed at 0.3 V/SCE but ferrocene oxidation peak is shifted to positive values while no reduction peak associated to the ferricinium reduction, is observed during backward scan. Such behavior indicates that the oligo(BTB) film is pinhole free and switches from insulating to conductive at 0.65 V/SCE<sup>29-30</sup>.

1  
2  
3 After the first oxidation cycle in presence of EDOT, the ferrocene signal on the new  
4 electrode is labelled “1” in Figure 1b. A typical diode like signature is still observed (Figure 1b  
5 curve 1), which indicates that the new electrode still switches from an insulating to a conductive  
6 state. However, the anodic peak potential is lowered compared to that observed on an  
7 unmodified BTB film. Upon further cycling, the anodic peak potential decreases more and after  
8 the third cycle, an emerging cathodic peak, corresponding to  $\text{Fc}^+$  reduction, is observed. The  
9 intensity of this cathodic peak increases progressively while the layer is modified during 3rd to  
10 7th cycle of EDOT oxidation. Simultaneously, the peak separation between anodic and cathodic  
11 peak, which is a measure of the reversible redox probe heterogeneous electron transfer kinetic  
12 constant, decreases. From the seventh cycle on, ferrocene shows reversible behaviour on the new  
13 organic electrode with  $\Delta E_p$  close to 60 mV and does not significantly changes upon further  
14 EDOT oxidation cycles.

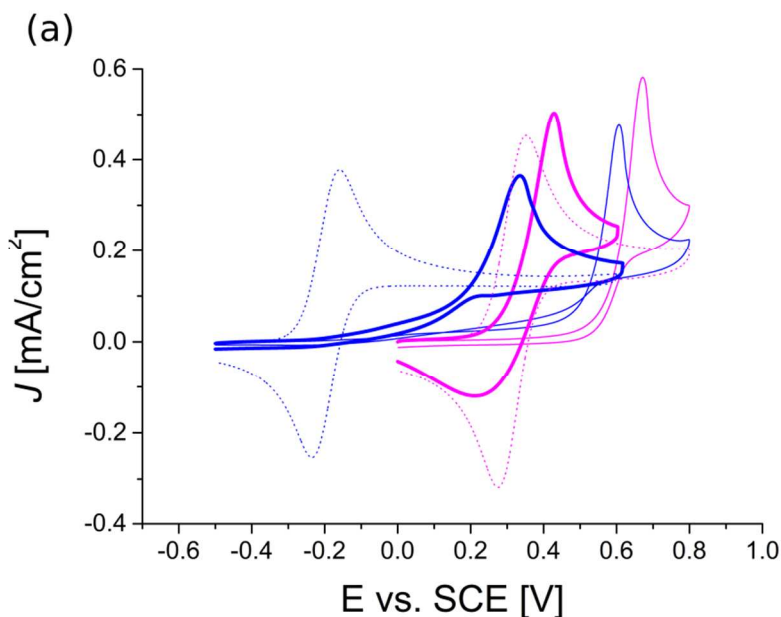
15  
16  
17  
18  
19  
20  
21  
22  
23  
24  
25  
26  
27  
28  
29  
30  
31  
32  
33 DmFc redox probe was also used to report on the transport properties of the layer after  
34 each EDOT oxidation cycle. The voltammograms obtained on DmFc are depicted in Figure 1c.  
35 They show a preserved diode-like behavior until the sixth cycle of EDOT oxidation, while after  
36 that, a growing cathodic signal appears, attributed to  $\text{DmFc}^+$  reduction on the modified electrode.  
37 Simultaneously  $\Delta E_p$  starts to get measurable at that point and decreases after each EDOT  
38 oxidation cycle and finally stabilises at 60 mV after nine successive EDOT cycles. After cycle 9,  
39 total reversibility is achieved also for DmFc. It is noticeable that at this moment, the film has  
40 become transparent towards Fc and DmFc.

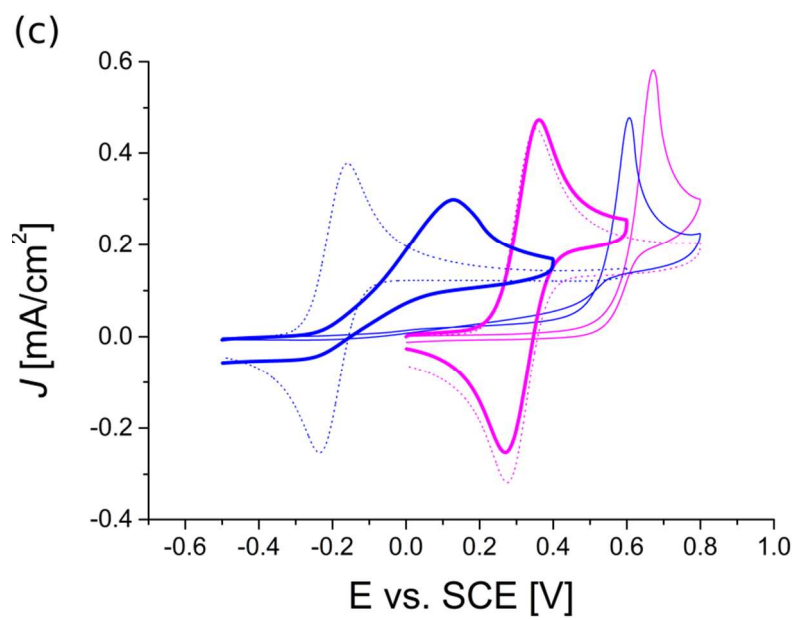
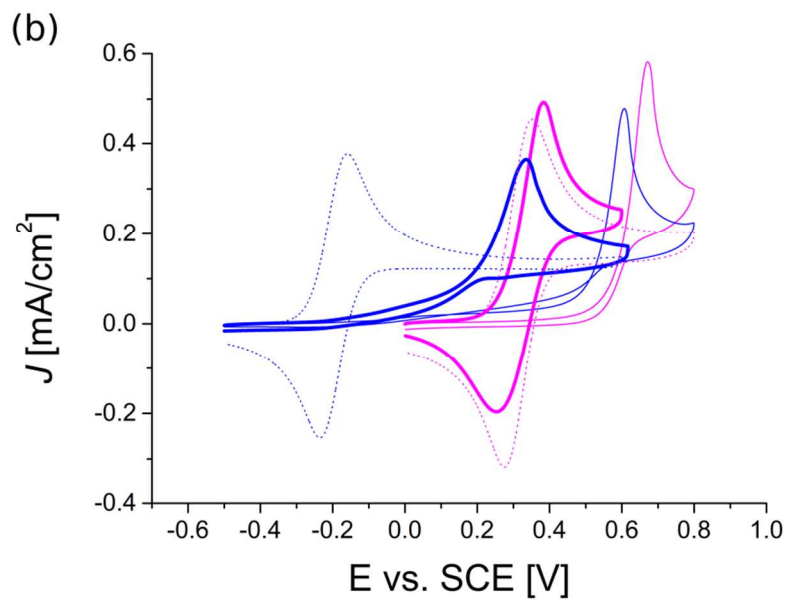
41  
42  
43  
44  
45  
46  
47  
48  
49  
50  
51  
52  
53 At that point, a first intermediate conclusion can be drawn. EDOT oxidation on  
54 oligo(BTB) layer chemically modifies the pristine oligo(BTB) layer and changes its transport  
55 properties. The shape of the electrochemical response of Fc and Dmfc clearly demonstrates that  
56  
57  
58  
59  
60

1  
2  
3 the new electrodes still switch from an insulating to a conductive state. The switching potential  
4 of EDOT modified BTB electrodes can be easily tuned from 0.65 V/SCE to below -0.3 V/SCE  
5 and at any intermediate values by careful control of the EDOT oxidation process. As a  
6 consequence, one can easily reach an intermediate situation in which EDOT modified  
7 oligo(BTB) electrode is transparent towards ferrocene, while a diode like behaviour is still  
8 observed with decamethylferrocene. This behaviour is expected from Scenario 1 (covalent  
9 grafting of oligo (EDOT) block on oligo(BTB)) as described in scheme 1 and is not compatible  
10 with scenario 2 in which the oligo(BTB) layer retain its switching potential. The differentiated  
11  $\Delta E_p$  evolution of Fc and DmFc redox probes associated to the pinhole free compact oligo(BTB)  
12 layer (observed in electrochemistry and when metal evaporation is directly performed on the  
13 layer) exclude PEDOT polymer growth through pinholes of the oligo(BTB) layer<sup>26, 36</sup>. As an  
14 important result, these experiments demonstrate that it is possible to tune the switching potential  
15 of the layer from its initial value of 0.65 V/SCE to below -0.3 V/SCE by using the procedure  
16 described above.  
17  
18  
19  
20  
21  
22  
23  
24  
25  
26  
27  
28  
29  
30  
31  
32  
33  
34  
35  
36

37 This distinctive evolution of the two redox probes signal is to our belief unique and has  
38 never been reported elsewhere. It is thus detailed in Figure 2 and Figure SII-X where X  
39 designates the number of EDOT oxidation cycles used to modify the BTB layer. Each figure also  
40 contains the electrochemical response of Fc and DmFc on a bare GC electrode and on the  
41 pristine oligo(BTB) film. By comparing both probe responses in one graph, we nicely see how  
42 their respective electrochemical signal gradually changes. After 1 cycle of EDOT oxidation  
43 (Figure SII-1), both redox probes show still irreversible behaviour while after cycle 2 (Figure  
44 2a), Fc already starts to exhibit a cathodic wave. After cycle 4, Fc finally starts to behave like on  
45 bare electrode (Figure 2b) and does not shift any more from cycle 6 on (Figure 2c), indicating  
46  
47  
48  
49  
50  
51  
52  
53  
54  
55  
56  
57  
58  
59  
60

1  
2  
3 that now, Fc is quasireversible on this film. In the meantime, DmFc still preserves its diode-like  
4 behavior and only after cycle 7 (Figure S11-7), a cathodic peak appears but the  $\Delta E_p$  is still  
5 superior to bare electrode, indicating that the electrode remains partially blocked<sup>37</sup>. After cycle 9  
6 (Figure 2d), both redox probes show reversible behaviour onto the modified electrode at the  
7 same  $E_0$  than on bare electrodes. Sonication in ACN during 15 minutes did not modify film  
8 responses, which is a further indication for covalent attachment of EDOT moieties and thus  
9 strongly points to Scenario 1 (scheme 1).  
10  
11  
12  
13  
14  
15  
16  
17  
18  
19  
20





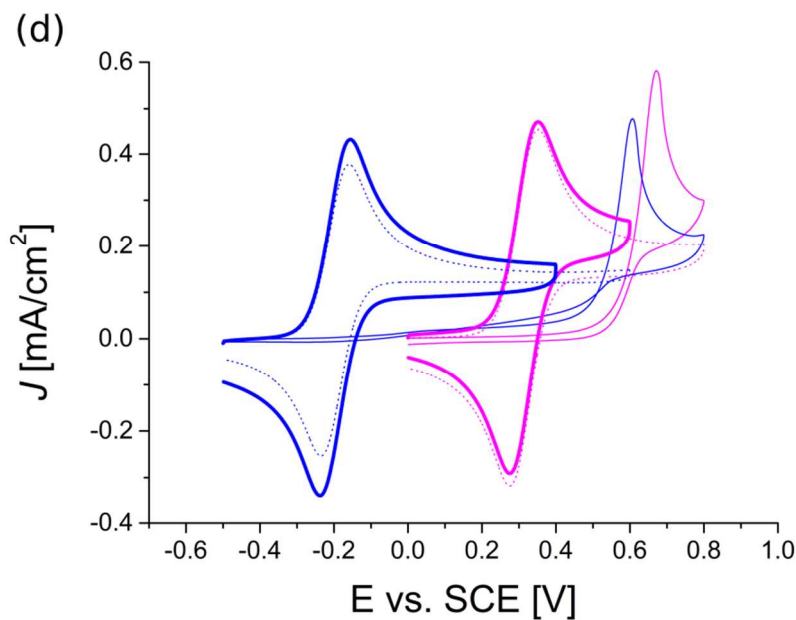


**Figure 2:** Comparison of Fc (pink line) and DmFc (blue line) (both at 1mM concentration in ACN with 0.1 M LiClO<sub>4</sub> as supporting electrolyte) response on oligo(BTB) modified electrodes (thin solid line) and after cycling in EDOT solution (2 x 10<sup>-2</sup> M) (dashed line) with redox probe response on bare glassy carbon electrode (thick solid line). (a) After 2 EDOT overgrafting cycles, (b) after 4 EDOT overgrafting cycles (c) after 6 EDOT overgrafting cycles, (d) after 9 overgrafting cycles. Scan rate: 0.1 V/s.

To characterize further the film modification, electroactivity of the EDOT-modified-BTB-electrode was recorded in ACN at 10 V/s with IR drop compensation (Figure 3a) after each EDOT oxidation cycle, and compared to that of an unmodified oligo(BTB) electrode. This electroactivity shows small anodic and cathodic peaks shifting progressively towards less positive values upon successive EDOT oxidation cycle. Initial anodic peak for BTB is above 0.75 V/SCE then shifts to 0.55, 0.50, 0.35, 0.25 and 0.15 V/SCE after 1, 3, 5, 7 and 8 EDOT oxidation cycles, respectively. Cathodic current peak follows the same tendency and the anodic current density onset also decreases to lower potential upon successive EDOT oxidation cycle.

These measurements confirm that the switching potential of the EDOT modified oligo(BTB) electrode is progressively lowered.

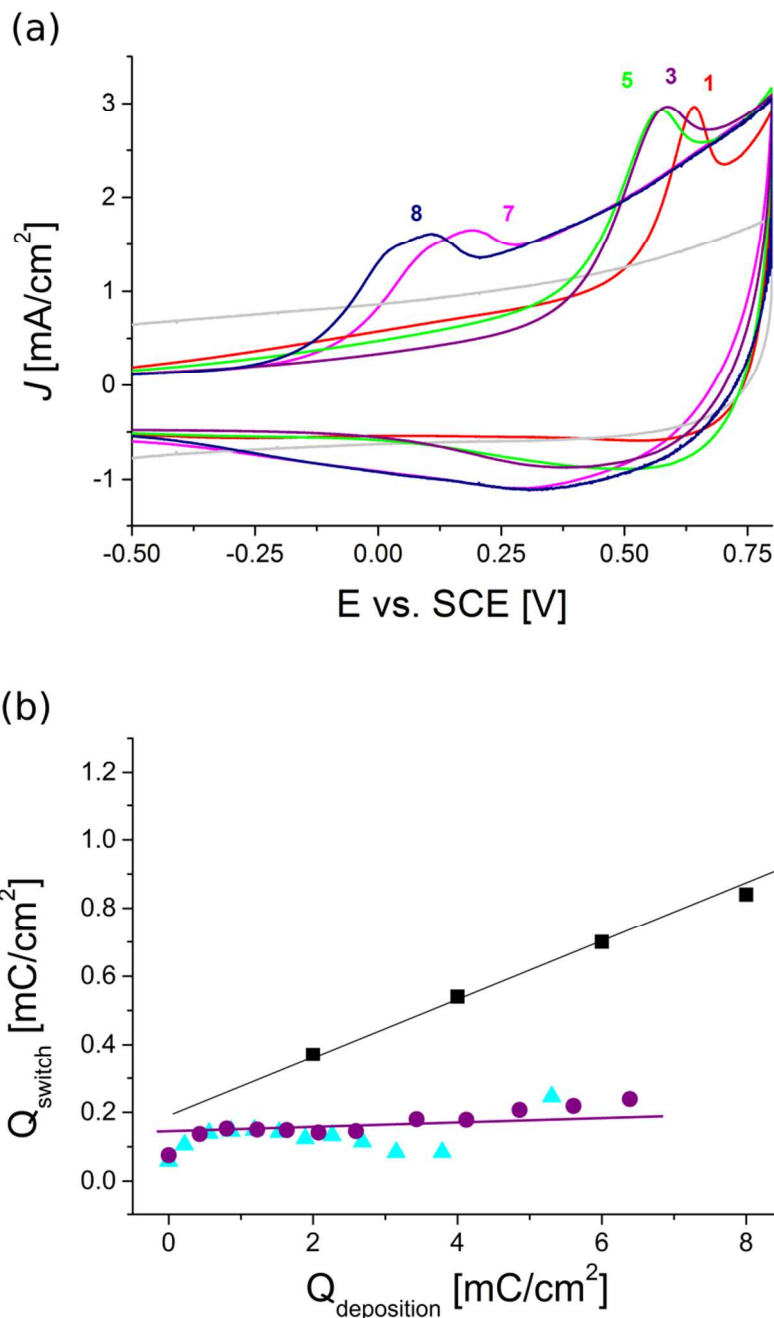


**Figure 3:** a) Electroactivity after 1, 3, 5, 7 and 8 EDOT oxidation cycle respectively on BTB-modified GC electrode. CVs are recorded in ACN with LiClO<sub>4</sub> (0.1 M) as supporting electrolyte. Grey line is bare electrode, scan rate: 10 V/s (ohmic drop correction). (b) Evolution of  $Q_{\text{switch}}$  as a

1  
2  
3 function of  $Q_{\text{deposition}}$ . Colours correspond to two different electrodes, black squares represent  
4 PEDOT deposition on bare electrode.  
5

6  
7 By integration of the CV, the amount of charge observed for doping the deposited layer  
8  
9 ( $Q_{\text{switch}}$ ) as a function of charge applied during EDOT anodic deposition ( $Q_{\text{deposition}}$ ) was  
10 determined.  $Q_{\text{switch}}$  was plotted against  $Q_{\text{deposition}}$  (Figure 3b blue and magenta points) and  
11 compared to the results obtained when anodic polymerisation of EDOT is performed on a bare  
12 electrode (Figure 3b black points), without underlying oligo(BTB) layer. On a bare GC  
13 electrode, a linear increase of  $Q_{\text{switch}}$  with a  $Q_{\text{deposition}}$  is observed with a ratio close to 10 between  
14  
15  $Q_{\text{deposition}}$  and  $Q_{\text{switch}}$ <sup>38-39</sup>. Such behaviour has already been observed for many conducting  
16  
17 polymers. When EDOT oxidation is performed on a oligo(BTB) layer, the evolution of  $Q_{\text{switch}}$  is  
18  
19 clearly different. It does not significantly increase upon the successive EDOT deposition cycle  
20  
21 and remains around  $0.2 \text{ mC/cm}^2$  ( $\Gamma = 2.10^{-9} \text{ mol/cm}^2$ ) when  $Q_{\text{deposition}}$  increases. However when  
22  
23  $Q_{\text{deposition}}$  gets above  $6.5 \text{ mC/cm}^2$ , the expected curve for PEDOT polymerisation is obtained as  
24  
25 can be seen in figure SI3. This result is a very strong indication that covalent grafting of few  
26  
27 EDOT units had taken place on the BTB oligomers yielding to a block oligo(BTB)-oligo(EDOT)  
28  
29 that can be oxidized at a lower potential compared to oligo(BTB). (Note also that under  
30  
31 application of this charge, a PEDOT film of around 30 nm would be formed if it was performed  
32  
33 on a bare electrode.)  
34  
35  
36  
37  
38  
39  
40  
41  
42  
43  
44

45  
46 In order to measure the thickness variation of the oligo(BTB) film upon EDOT oxidation,  
47  
48 similar experiments were performed on gold stripes,  $42 \pm 0.5 \text{ nm}$  thick, e-beam deposited on  
49  
50 Si/SiO<sub>2</sub> substrates. This allows to use AFM for thickness measurements at each step of the  
51  
52 electrochemical bottom up process. As the stripes exhibit a very small size of  $20 \text{ }\mu\text{m}$  per  $5 \text{ mm}$ ,  
53  
54 the electrochemical response of ferrocene is close to that obtained on an ultramicroelectrode  
55  
56 (UME) with stationary plateau currents observed when ferrocene is oxidized to ferricinium.<sup>28-29</sup>  
57  
58  
59  
60

1  
2  
3  
4  
5  
6  
7  
8  
9  
10  
11  
12  
13  
14  
15  
16  
17  
18  
19  
20  
21  
22  
23  
24  
25  
26  
27  
28  
29  
30  
31  
32  
33  
34  
35  
36  
37  
38  
39  
40  
41  
42  
43  
44  
45  
46  
47  
48  
49  
50  
51  
52  
53  
54  
55  
56  
57  
58  
59  
60

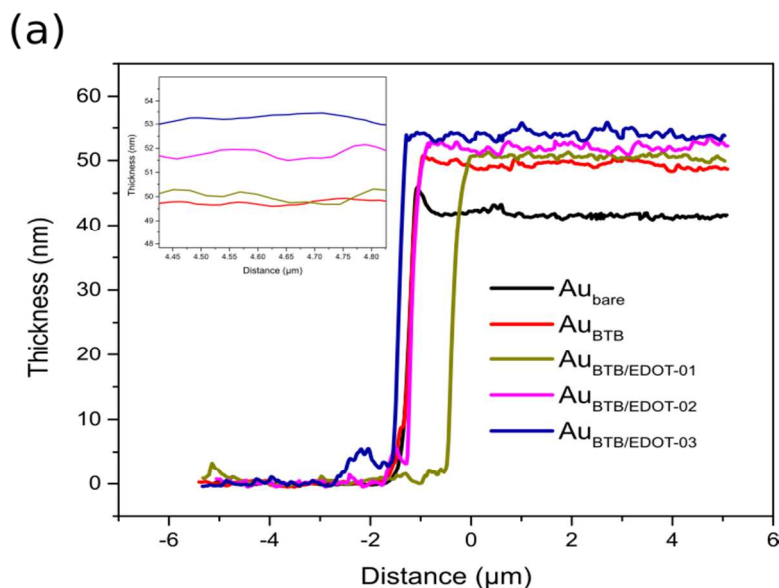
Figure 4a shows the AFM profile of three different films generated on gold stripes while Figure 4b and 4c show the behaviour of ferrocene and decamethylferrocene on these electrodes. The first one is a oligo(BTB) electrode and Figure 4a reveals that the oligo(BTB) exhibits an average thickness of 7.5-8 nm with a root mean square roughness of 0.7 nm. As expected on the gold/BTB electrode, the electrochemical oxidation of Fc and DmcFe is shifted to 0.7 V/SCE whereas on a bare electrode, a plateau like current at 0.3 V/SCE and -0.2 V/SCE is observed. Note also that the value of the diffusion limited current is the same on the bare and all modified electrodes.

The oligo(BTB) electrode was then modified by EDOT oxidation, generating a new modified electrode labelled BTB-EDOT1. The thickness of the organic layer is close to 9 nm and the roughness of this electrode appears almost the same as that of the initial oligo(BTB) electrode. However, the Fc and response on this electrode is significantly different with an onset for ferrocene oxidation at 0.3 V/SCE, a current rising on a larger potential range and a plateau current obtained only at 0.5 V/SCE. This result shows that despite a minimal amount of EDOT grafted on the BTB oligomers (around one nm thickness increase, i.e. 1 or 2 EDOT moieties), the switching potential of the new BTB-EDOT1 electrode decreases sharply from its initial value. This result is compatible with that observed when films are generated from new diazonium cations, derived from 2-(4-aminophenyl)-3,4-ethylenedioxy-thiophene and various amino-functionalized  $\pi$ -conjugated oligomers incorporating 3,4-ethylenedioxythiophene (EDOT) and thiophene units<sup>30</sup>.

A second electrode labelled BTB-EDOT2 was then generated and studied. Its thickness is now 9-10 nm with a roughness of 0.9 nm. EDOT block of the electrode is thus only 2 to 3 nm which implies that the EDOT block grafted on the oligo(BTB) electrode consists of only 4 to 6

1  
2  
3 EDOT units. Fc signal on this electrode is at the same potential and has the same shape as on a  
4 bare gold stripe, showing that BTB-EDOT2 electrode has a switching potential below the  
5  
6 bare gold stripe, showing that BTB-EDOT2 electrode has a switching potential below the  
7  
8 standard redox potential of ferrocene. On the contrary, DmFc signal is still shifted to higher  
9  
10 potential when compared to its position on a bare gold stripe. Onset of DmFc oxidation signal is  
11  
12 now at 0.0 V/SCE and plateau current is reached at 0.2 V/SCE which is as expected below the  
13  
14 standard redox potential of Fc.  
15  
16

17  
18  
19 Finally, a third electrode labelled BTB-EDOT3 was generated. The thickness of the  
20  
21 organic layer is 10-11 nm with an average roughness of 1.1 nm and this electrode is transparent  
22  
23 for ferrocene but not yet fully transparent for DmFc as DmFc oxidation onset is seen at -0.1  
24  
25 V/SCE with plateau current reached at 0V/SCE. Thickness measurements indicate that the  
26  
27 oligo(EDOT) block grafted on the initial oligo(BTB) units is only 3-4 nm thick that is close to 6  
28  
29 to 8 EDOT units.  
30  
31  
32  
33  
34



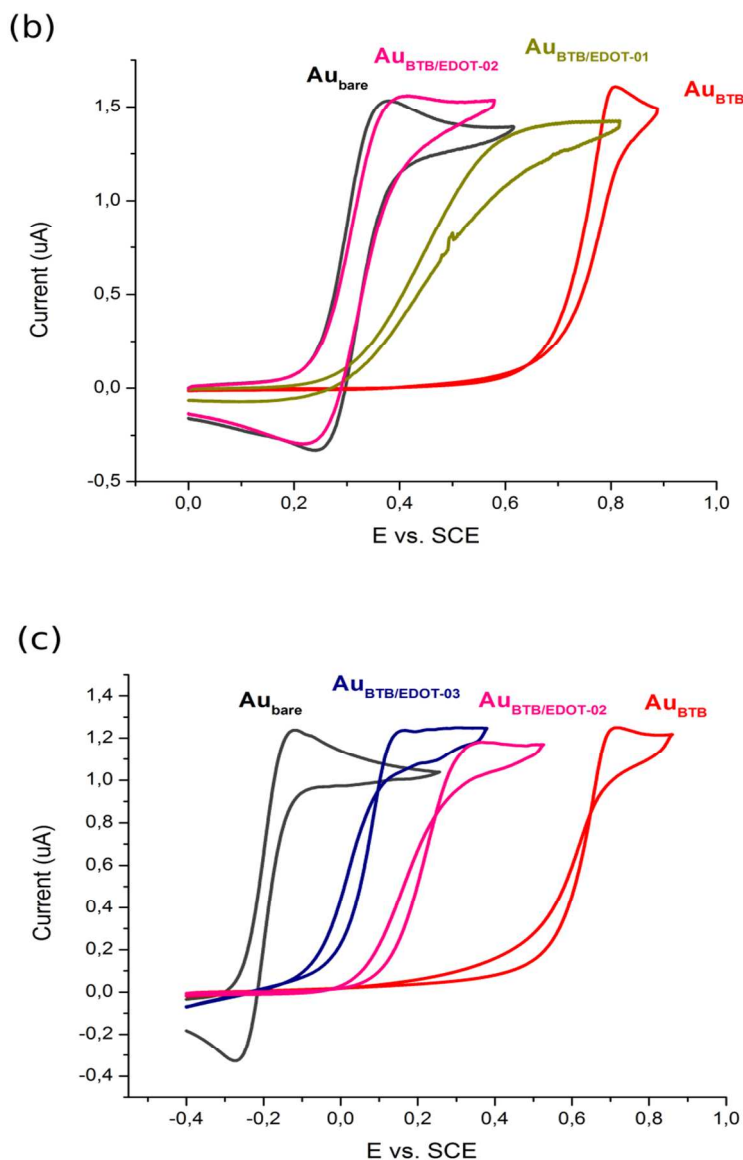
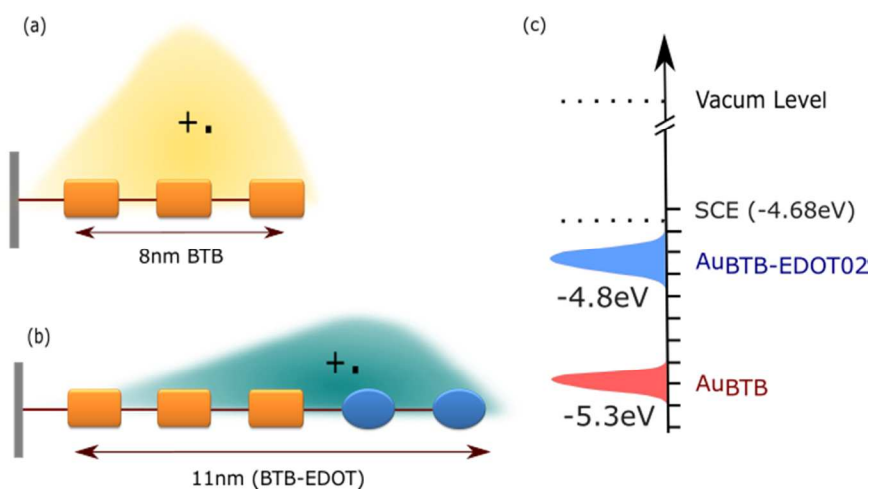


**Figure 4:** a) AFM profiles of a gold stripe covered with various organic layers. Bare gold, Gold-BTB and Gold-BTB-EDOT1, Gold-BTB-EDOT2 and Gold-BTB-EDOT3 electrodes obtained by successive EDOT oxidation cycles at low current densities on the BTB-gold electrode. Note that the results reported here are obtained on a unique electrode that is modified in several successive steps. b) 3D AFM image of a Gold-BTB-EDOT3 electrode c) Response of ferrocene on the BTB-EDOT modified electrodes (1 mM) with LiClO<sub>4</sub> (0.1 M) as supporting electrolyte in ACN, (d) Response of decamethylferrocene on the same BTB-EDOT modified electrodes (1 mM) with LiClO<sub>4</sub> (0.1 M) as supporting electrolyte in ACN.

Overall, Scheme 2 summarizes the finding of this work. Starting from and 8 nm oligo(BTB) layer acting as a switchable electrode, it is possible to create a large set of new

1  
2  
3 materials with tunable electrochemical properties. Oligo(EDOT) block of various length are  
4 grafted on the oligo(BTB) moieties leading to chain extension. As a consequence the new  
5 oligomers have higher energy HOMOs as seen in scheme 2c and the layer can switch from a  
6 conductive to insulating state at lower potential than the initial oligo(BTB) electrode. As long as  
7  
8 oligomers have higher energy HOMOs as seen in scheme 2c and the layer can switch from a  
9  
10 conductive to insulating state at lower potential than the initial oligo(BTB) electrode. As long as  
11  
12 the overall thickness remains below 11 nm, the charge involved in the film electroactivity  
13  
14 remains that of the initial oligo(BTB) layer with polaron, spreading over most of the oligomer<sup>40</sup>,  
15  
16 likely localized on the growing EDOT block as depicted in Scheme 2b. Ultimately further growth  
17  
18 will generate PEDOT chains on the electrodes as observed in figure SI3. This set of new material  
19  
20 with tunable switching properties through a bottom-up electrochemical process leading to  
21  
22 ultrathin layers with tailored switchable properties.  
23  
24  
25  
26



27  
28  
29  
30  
31  
32  
33  
34  
35  
36  
37  
38  
39  
40  
41  
42  
43  
44  
45  
46  
47  
48  
49  
50  
51  
52  
53  
54  
55  
56  
57  
58  
59  
60

Scheme 2: Overall evolutions of the organic electrode properties while grafting 3 nm of oligo(EDOT) block on an 8 nm thick oligo(BTB) organic electrode. The yellow and green envelopes represent the plausible extension a polaron on each oligomer.

## CONCLUSION

1  
2  
3 In this work, focus was set towards extending the properties of ultrathin electroactive layers,  
4 based on oligo(BTB) layer, covalently attached to the electrode by diazonium salt reduction.  
5  
6 Such layers switch from an insulating, to a conductive state and acts above their switching  
7 potential as organic electrodes This switch is strongly dependent on the molecular structure of  
8 the diazonium salt precursor. Here, EDOT oxidation was performed on ultrathin oligo(BTB)  
9 layers. We show first that EDOT can be easily oxidized on such organic electrode and that by  
10 using small current densities, EDOT oxidation does not generate PEDOT film on the oligo(BTB)  
11 layer but oligo(EDOT) oligomers grafted covalently on the oligo(BTB) units. As a consequence,  
12 new elongated oligomers with a block structure are generated on the surface. Moreover, the  
13 degree of elongation can be easily controlled as we observe successive switching potential  
14 decrease as a function of the EDOT overgrafting cycles, evidenced in voltammograms recorded  
15 in presence of several redox probes with different redox potentials. Depending on the length of  
16 the oligo(EDOT) block, the switching potential of the new layers can be tuned at will from 0.6  
17 V/SCE to  $-0.3$  V/SCE. As an exciting result, these large switching potential variations are  
18 obtained by grafting less than 3-4 nm of oligo(EDOT) on the oligo(BTB) layer.  
19  
20  
21  
22  
23  
24  
25  
26  
27  
28  
29  
30  
31  
32  
33  
34  
35  
36  
37  
38

39 Overall, a bottom-up electrochemical process for oligomer elongation is indeed possible  
40 and leads to thin films with very low switching potential being covalently grafted to the electrode  
41 surface. Furthermore, film switching potential can be fine-tuned to the desired potential,  
42 facilitating device fabrication. Finally, overgrafting electron withdrawing groups by a similar  
43 procedure, is likely to raise the switching potential of the layer instead of decreasing it, a feature  
44 which could enlarge even more the possibilities for tailoring film switching potentials to any  
45 desired potential. Such experiments are under investigation.  
46  
47  
48  
49  
50  
51  
52  
53  
54  
55  
56  
57  
58  
59  
60

## ASSOCIATED CONTENT

**Supporting Information.** Comparison of Fc and DmFc response on oligo(BTB) modified electrodes and after cycling in EDOT solution after 1 and 7 EDOT overgrafting cycle, Evolution of  $Q_{\text{switch}}$  as a function of  $Q_{\text{deposition}}$  when.  $Q_{\text{deposition}}$  is above  $7 \text{ mC/cm}^2$ . This material is available free of charge via the Internet at <http://pubs.acs.org>.”

## AUTHOR INFORMATION

**Corresponding Author**

\* [lacroix@univ-paris-diderot.fr](mailto:lacroix@univ-paris-diderot.fr)

**Notes**

The authors declare no competing financial interest

## ACKNOWLEDGMENT

This work was supported by the CNRS, the University Paris Diderot (Paris, France) and by a Ph.D. grant from the University of Science and Technology of Hanoi.

## REFERENCES

1. Magasinski, A.; Dixon, P.; Hertzberg, B.; Kvit, A.; Ayala, J.; Yushin, G., High-performance lithium-ion anodes using a hierarchical bottom-up approach. *Nat Mater* **2010**, *9* (4), 353-358.
2. Godeau, G.; Darmanin, T.; Guittard, F., Switchable surfaces from highly hydrophobic to highly hydrophilic using covalent imine bonds. *J Appl Polym Sci* **2016**, *133* (11), n/a-n/a.
3. Wang, J.; Li, J.; Li, N.; Guo, X.; He, L.; Cao, X.; Zhang, W.; He, R.; Qian, Z.; Cao, Y.; Chen, Y., A Bottom-Up Approach to Dual Shape-Memory Effects. *Chem Mater* **2015**, *27* (7), 2439-2448.
4. Santos, L.; Martin, P.; Ghilane, J.; Lacaze, P. C.; Lacroix, J.-C., Micro/Nano-Structured Polypyrrole Surfaces on Oxidizable Metals as Smart Electroswitchable Coatings. *ACS Applied Materials & Interfaces* **2013**, *5* (20), 10159-10164.

5. Lee, L.; Gunby, N. R.; Crittenden, D. L.; Downard, A. J., Multifunctional and Stable Monolayers on Carbon: A Simple and Reliable Method for Backfilling Sparse Layers Grafted from Protected Aryldiazonium Ions. *Langmuir* **2016**, *32* (11), 2626-2637.
6. Lee, L.; Leroux, Y. R.; Hapiot, P.; Downard, A. J., Amine-Terminated Monolayers on Carbon: Preparation, Characterization, and Coupling Reactions. *Langmuir* **2015**, *31* (18), 5071-5077.
7. Xu, L.; Chen, W.; Mulchandani, A.; Yan, Y., Reversible Conversion of Conducting Polymer Films from Superhydrophobic to Superhydrophilic. *Angew Chem Int Ed* **2005**, *44* (37), 6009-6012.
8. Hermelin, E.; Petitjean, J.; Lacroix, J.-C.; Chane-Ching, K. I.; Tanguy, J.; Lacaze, P.-C., Ultrafast Electrosynthesis of High Hydrophobic Polypyrrole Coatings on a Zinc Electrode: Applications to the Protection against Corrosion. *Chem Mater* **2008**, *20* (13), 4447-4456.
9. Wang, X.; Berggren, M.; Inganäs, O., Dynamic Control of Surface Energy and Topography of Microstructured Conducting Polymer Films. *Langmuir* **2008**, *24* (11), 5942-5948.
10. Xu, L.; Wang, J.; Song, Y.; Jiang, L., Electrically Tunable Polypyrrole Inverse Opals with Switchable Stopband, Conductivity, and Wettability. *Chem Mater* **2008**, *20* (11), 3554-3556.
11. Santos, L. M.; Ghilane, J.; Fave, C.; Lacaze, P. C.; Randriamahazaka, H.; Abrantes, L. M.; Lacroix, J. C., Electrografting polyaniline on carbon through the electroreduction of diazonium salts and the electrochemical polymerization of aniline. *Journal of Physical Chemistry C* **2008**, *112*, 16103-16109.
12. Nguyen, V.-Q.; Schaming, D.; Martin, P.; Lacroix, J.-C., Highly Resolved Nanostructured PEDOT on Large Areas by Nanosphere Lithography and Electrodeposition. *ACS Applied Materials & Interfaces* **2015**, *7* (39), 21673-21681.
13. Santos, L.; Ghilane, J.; Lacroix, J. C., Formation of Mixed Organic Layers by Stepwise Electrochemical Reduction of Diazonium Compounds. *J Am Chem Soc* **2012**, *134* (12), 5476-5479.
14. Jacques, A.; Barthélémy, B.; Delhalle, J.; Mekhalif, Z., 1-Pyrrolyl-10-decylammoniumphosphonate monolayer: a molecular nanolink between electropolymerized pyrrole films and nickel or titanium surfaces. *Electrochim Acta* **2015**, *170*, 218-228.
15. Lu, W.; Lieber, C. M., Nanoelectronics from the bottom up. *Nat Mater* **2007**, *6* (11), 841-850.
16. Love, J. C.; Estroff, L. A.; Kriebel, J. K.; Nuzzo, R. G.; Whitesides, G. M., Self-Assembled Monolayers of Thiolates on Metals as a Form of Nanotechnology. *Chem Rev* **2005**, *105* (4), 1103-1170.
17. McCreery, R. L., Molecular Electronic Junctions. *Chem Mater* **2004**, *16* (23), 4477-4496.
18. Sedghi, G.; García-Suárez, V. M.; Esdaile, L. J.; Anderson, H. L.; Lambert, C. J.; Martín, S.; Bethell, D.; Higgins, S. J.; Elliott, M.; Bennett, N.; Macdonald, J. E.; Nichols, R. J., Long-range electron tunnelling in oligo-porphyrin molecular wires. *Nature nanotechnology* **2011**, *6* (July), 517-523.
19. Yan, H.; Berggren, A. J.; McCreery, R.; Della Rocca, M. L.; Martin, P.; Lafarge, P.; Lacroix, J. C., Activationless charge transport across 4.5 to 22 nm in molecular electronic junctions. *Proc Natl Acad Sci U S A* **2013**, *110* (14), 5326-30.
20. Yuan, L.; Breuer, R.; Jiang, L.; Schmittl, M.; Nijhuis, C. a., A Molecular Diode with a Statistically Robust Rectification Ratio of Three Orders of Magnitude. *Nano Lett* **2015**, 150721171048008-150721171048008.

21. Ho Choi, S.; Kim, B.; Frisbie, C. D., Electrical Resistance of Long Conjugated Molecular Wires. *Science* **2008**, *320* (5882), 1482-1486.
22. Tran, E.; Duati, M.; Ferri, V.; Müllen, K.; Zharnikov, M.; Whitesides, G. M.; Rampi, M. A., Experimental Approaches for Controlling Current Flowing through Metal–Molecule–Metal Junctions. *Adv Mater* **2006**, *18* (10), 1323-1328.
23. Tuccitto, N.; Ferri, V.; Cavazzini, M.; Quici, S.; Zhavnerko, G.; Licciardello, A.; Rampi, M. A., Highly conductive [sim]40-nm-long molecular wires assembled by stepwise incorporation of metal centres. *Nat Mater* **2009**, *8* (1), 41-46.
24. Choi, S. H.; Risko, C.; Delgado, M. C. R.; Kim, B.; Brédas, J.-L.; Frisbie, C. D., Transition from Tunneling to Hopping Transport in Long, Conjugated Oligo-imine Wires Connected to Metals. *J Am Chem Soc* **2010**, *132* (12), 4358-4368.
25. McCreery, R. L.; Yan, H.; Bergren, A. J., A critical perspective on molecular electronic junctions: there is plenty of room in the middle. *PCCP* **2013**, *15* (4), 1065-1081.
26. Martin, P.; Della Rocca, M. L.; Anthore, A.; Lafarge, P.; Lacroix, J.-C., Organic Electrodes Based on Grafted Oligothiophene Units in Ultrathin, Large-Area Molecular Junctions. *J Am Chem Soc* **2012**, *134* (1), 154-157.
27. Sayed, S. Y.; Bayat, A.; Kondratenko, M.; Leroux, Y.; Hapiot, P.; McCreery, R. L., Bilayer Molecular Electronics: All-Carbon Electronic Junctions Containing Molecular Bilayers Made with “Click” Chemistry. *J Am Chem Soc* **2013**, *135* (35), 12972-12975.
28. Fave, C.; Leroux, Y.; Trippé, G.; Randriamahazaka, H.; Noel, V.; Lacroix, J.-C., Tunable Electrochemical Switches Based on Ultrathin Organic Films. *J Am Chem Soc* **2007**, *129* (7), 1890-1891.
29. Fave, C.; Noel, V.; Ghilane, J.; Trippé-Allard, G.; Randriamahazaka, H.; Lacroix, J. C., Electrochemical Switches Based on Ultrathin Organic Films: From Diode-like Behavior to Charge Transfer Transparency. *J. Phys. Chem. C* **2008**, *112* (47), 18638-18643.
30. Stockhausen, V.; Trippé-Allard, G.; Van Quynh, N.; Ghilane, J.; Lacroix, J.-C., Grafting  $\pi$ -Conjugated Oligomers Incorporating 3,4-Ethylenedioxythiophene (EDOT) and Thiophene Units on Surfaces by Diazonium Electroreduction. *J. Phys. Chem. C* **2015**, *119* (33), 19218-19227.
31. Stockhausen, V.; Ghilane, J.; Martin, P.; Trippé-Allard, G.; Randriamahazaka, H.; Lacroix, J.-C., Grafting Oligothiophenes on Surfaces by Diazonium Electroreduction: A Step toward Ultrathin Junction with Well-Defined Metal/Oligomer Interface. *J Am Chem Soc* **2009**, *131* (41), 14920-14927.
32. Trippé-Allard, G.; Lacroix, J.-C., Synthesis of nitro- and amino-functionalized  $\pi$ -conjugated oligomers incorporating 3,4-ethylenedioxythiophene (EDOT) units. *Tetrahedron* **2013**, *69* (2), 861-866.
33. Doyle, M. P.; Bryker, W. J., Alkyl nitrite-metal halide deamination reactions. 6. Direct synthesis of arenediazonium tetrafluoroborate salts from aromatic amines, tert-butyl nitrite, and boron trifluoride etherate in anhydrous media. *The Journal of Organic Chemistry* **1979**, *44* (9), 1572-1574.
34. Delamar, M.; Hitmi, R.; Pinson, J.; Saveant, J. M., Covalent modification of carbon surfaces by grafting of functionalized aryl radicals produced from electrochemical reduction of diazonium salts. *J Am Chem Soc* **1992**, *114* (14), 5883-5884.
35. Baranton, S.; Bélanger, D., In situ generation of diazonium cations in organic electrolyte for electrochemical modification of electrode surface. *Electrochim Acta* **2008**, *53* (23), 6961-6967.

- 1  
2  
3  
4  
5  
6  
7  
8  
9  
10  
11  
12  
13  
14  
15  
16  
17  
18  
19  
20  
21  
22  
23  
24  
25  
26  
27  
28  
29  
30  
31  
32  
33  
34  
35  
36  
37  
38  
39  
40  
41  
42  
43  
44  
45  
46  
47  
48  
49  
50  
51  
52  
53  
54  
55  
56  
57  
58  
59  
60
36. Fluteau, T.; Bessis, C.; Barraud, C.; Della Rocca, M. L.; Martin, P.; Lacroix, J.-C.; Lafarge, P., Tuning the thickness of electrochemically grafted layers in large area molecular junctions. *J Appl Phys* **2014**, *116* (11), 114509.
37. Amatore, C.; Savéant, J. M.; Tessier, D., Charge transfer at partially blocked surfaces. *Journal of Electroanalytical Chemistry and Interfacial Electrochemistry* **1983**, *147* (1), 39-51.
38. LaCroix, J. C.; Diaz, A. F., Electrolyte Effects on the Switching Reaction of Polyaniline. *J Electrochem Soc* **1988**, *135* (6), 1457-1463.
39. Dung Nguyen, T.; Camalet, J. L.; Lacroix, J. C.; Aeiyaich, S.; Pham, M. C.; Lacaze, P. C., Polyaniline electrodeposition from neutral aqueous media: Application to the deposition on oxidizable metals. *Synth Met* **1999**, *102* (1), 1388-1389.
40. Lacroix, J. C.; Chane-Ching, K. I.; Maquère, F.; Maurel, F., Intrachain Electron Transfer in Conducting Oligomers and Polymers: The Mixed Valence Approach. *J Am Chem Soc* **2006**, *128* (22), 7264-7276.

Insert Table of Contents Graphic and Synopsis Here

